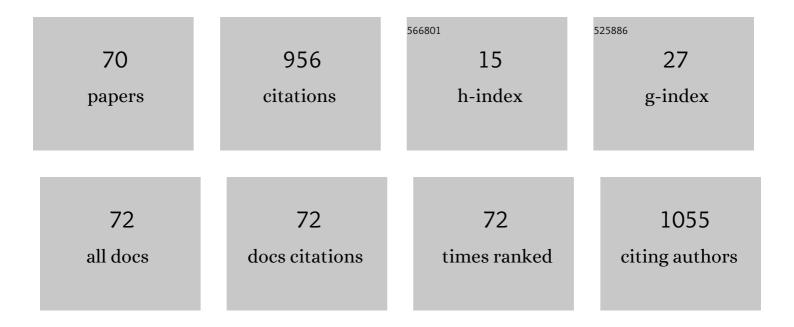
## Nenad Velisavljevic

List of Publications by Year in descending order

Source: https://exaly.com/author-pdf/1913543/publications.pdf Version: 2024-02-01



#	Article	IF	CITATIONS
1	Hydrostatic Compression Curve for Triaminoâ€Trinitrobenzene Determined to 13.0â€GPa with Powder Xâ€Ray Diffraction. Propellants, Explosives, Pyrotechnics, 2008, 33, 286-295.	1.0	103
2	Pressure induced structural transitions in CuSbS2 and CuSbSe2 thermoelectric compounds. Journal of Alloys and Compounds, 2015, 643, 186-194.	2.8	54
3	Strong, Ductile, and Thermally Stable bcc-Mg Nanolaminates. Scientific Reports, 2017, 7, 8264.	1.6	53
4	Distortion of alpha-uranium structure in praseodymium metal to 311ÂGPA. High Pressure Research, 2004, 24, 295-302.	0.4	44
5	A high-pressure far- and mid-infrared study of 1,1-diamino-2,2-dinitroethylene. Journal of Applied Physics, 2012, 111, .	1.1	37
6	The phase diagram of ammonium nitrate. Journal of Chemical Physics, 2012, 137, 064504.	1.2	36
7	1,1-diamino-2,2-dinitroethylene under high pressure-temperature. Journal of Chemical Physics, 2012, 137, 174304.	1.2	35
8	High Pressure–Temperature Phase Diagram of 1,1-Diamino-2,2-dinitroethylene (FOX-7). Journal of Physical Chemistry A, 2015, 119, 9739-9747.	1.1	32
9	Crystal grain growth at thel±-uranium phase transformation in praseodymium. Physical Review B, 2005, 71, .	1.1	30
10	Electrical measurements on praseodymium metal to 179 GPa using designer diamond anvils. Applied Physics Letters, 2004, 84, 927-929.	1.5	29
11	Structural and electrical properties of beryllium metal to 66 GPa studied using designer diamond anvils. Physical Review B, 2002, 65, .	1.1	27
12	Intermolecular Stabilization of 3,3′-Diamino-4,4′-azoxyfurazan (DAAF) Compressed to 20 GPa. Journal of Physical Chemistry A, 2014, 118, 5969-5982.	1.1	25
13	Novel experimental setup for megahertz X-ray diffraction in a diamond anvil cell at the High Energy Density (HED) instrument of the European X-ray Free-Electron Laser (EuXFEL). Journal of Synchrotron Radiation, 2021, 28, 688-706.	1.0	21
14	Effects of interstitial impurities on the high pressure martensitic α to ω structural transformation and grain growth in zirconium. Journal of Physics Condensed Matter, 2011, 23, 125402.	0.7	20
15	Bioceramic hydroxyapatite at high pressures. Applied Physics Letters, 2003, 82, 4271-4273.	1.5	17
16	Direct hcp→bcc structural phase transition observed in titanium alloy at high pressure. Applied Physics Letters, 2007, 91, .	1.5	16
17	High-Pressure Raman Spectroscopy and X-ray Diffraction Studies of a Terpolymer of Tetrafluoroethylene-Hexafluoropropylene-Vinylidene Fluoride: THV 500. Applied Spectroscopy, 2008, 62, 142-148.	1.2	16
18	The high-pressure phase behavior and compressibility of 2,4,6-trinitrotoluene. Applied Physics Letters, 2008, 93, .	1.5	16

NENAD VELISAVLJEVIC

#	Article	IF	CITATIONS
19	Pressure-induced kinetics of the <i>α</i> to <i>ï‰</i> transition in zirconium. Journal of Applied Physics, 2015, 118, .	1.1	16
20	X-ray Free Electron Laser-Induced Synthesis of ε-Iron Nitride at High Pressures. Journal of Physical Chemistry Letters, 2021, 12, 3246-3252.	2.1	14
21	Physical and mechanical properties of C60under high pressures and high temperatures. High Pressure Research, 2006, 26, 175-183.	0.4	13
22	High-pressure structural parameters and equation of state of osmium to 207ÂGPa. Cogent Physics, 2017, 4, 1376899.	0.7	13
23	Time-resolved x-ray diffraction and electrical resistance measurements of structural phase transitions in zirconium. Journal of Physics: Conference Series, 2014, 500, 032020.	0.3	12
24	High pressure studies using two-stage diamond micro-anvils grown by chemical vapor deposition. High Pressure Research, 2015, 35, 282-288.	0.4	12
25	Compressibility and thermoelectric behavior of TiCoSb half-Heusler compound at high pressures. Intermetallics, 2018, 95, 137-143.	1.8	12
26	Pressure-Induced Enhancement of Thermoelectric Figure of Merit and Structural Phase Transition in TiNiSn. Journal of Physical Chemistry Letters, 2021, 12, 1046-1051.	2.1	12
27	Structural phase stability in nanocrystalline titanium to 161 GPa. Materials Research Express, 2014, 1, 035044.	0.8	11
28	High-pressure high-temperature synthesis and thermal equation of state of high-entropy transition metal boride. AIP Advances, 2021, 11, .	0.6	11
29	Isotopically pure C13 layer as a stress sensor in a diamond anvil cell. Applied Physics Letters, 2004, 84, 5308-5310.	1.5	10
30	Thermal equation of state and thermodynamic Grüneisen parameter of beryllium metal. Journal of Applied Physics, 2013, 114, .	1.1	10
31	Ultrahigh pressure equation of state of tantalum to 310â€GPa. High Pressure Research, 2019, 39, 489-498.	0.4	10
32	Structure and properties of pseudomorphically transformed bcc Mg in Mg/Nb multilayered nanolaminates studied using synchrotron X-ray diffraction. Journal of Applied Physics, 2019, 126, 025302.	1.1	10
33	Experimental melting curve of zirconium metal to 37 GPa. Journal of Physics Condensed Matter, 2020, 32, 355402.	0.7	10
34	Dynamic experiments to study the αâ^'ε phase transition in cerium. Journal of Applied Physics, 2020, 127, 095901.	1.1	10
35	Simultaneous electrical and X-ray diffraction studies on neodymium metal to 152ÂGPa. High Pressure Research, 2005, 25, 137-144.	0.4	9
36	Calibration of an isotopically enriched carbon-13 layer pressure sensor to 156GPa in a diamond anvil cell. Journal of Applied Physics, 2006, 99, 064906.	1.1	9

NENAD VELISAVLJEVIC

#	Article	IF	CITATIONS
37	High pressure-temperature polymorphism of 1,1-diamino-2,2-dinitroethylene. Journal of Physics: Conference Series, 2014, 500, 052005.	0.3	9
38	A broadband wavelet implementation for rapid ultrasound pulse-echo time-of-flight measurements. Review of Scientific Instruments, 2020, 91, 075115.	0.6	9
39	Room-temperature compression and equation of state of body-centered cubic zirconium. Journal of Physics Condensed Matter, 2020, 32, 12LT02.	0.7	9
40	Giant Pressureâ€Induced Enhancement of Seebeck Coefficient and Thermoelectric Efficiency in SnTe. ChemPhysChem, 2017, 18, 3315-3319.	1.0	8
41	High pressure and temperature equation of state and spectroscopic study of CeO <sub>2</sub> . Journal of Physics Condensed Matter, 2016, 28, 155401.	0.7	7
42	High-pressure Seebeck coefficients and thermoelectric behaviors of Bi and PbTe measured using a Paris-Edinburgh cell. Journal of Synchrotron Radiation, 2016, 23, 1368-1378.	1.0	7
43	Shear-driven instability in zirconium at high pressure and temperature and its relationship to phase-boundary behaviors. Physical Review B, 2017, 95, .	1.1	7
44	Mechanisms of Pressure-Induced Phase Transitions by Real-Time Laue Diffraction. Crystals, 2019, 9, 672.	1.0	7
45	High-Entropy Borides under Extreme Environment of Pressures and Temperatures. Materials, 2022, 15, 3239.	1.3	7
46	Nontrivial nanostructure, stress relaxation mechanisms, and crystallography for pressure-induced Si-l → Si-ll phase transformation. Nature Communications, 2022, 13, 982.	5.8	6
47	Nanocrystalline diamond micro-anvil grown on single crystal diamond as a generator of ultra-high pressures. AIP Advances, 2016, 6, 095027.	0.6	5
48	High pressure elasticity and thermal properties of depleted uranium. Journal of Applied Physics, 2016, 119, .	1.1	5
49	High-pressure X-ray diffraction and vibrational spectroscopy of polyethylene: Evidence for a structural phase transition. Vibrational Spectroscopy, 2020, 111, 103173.	1.2	5
50	EQUATION OF STATE OF AMMONIUM NITRATE. , 2009, , .		4
51	Titanium Alloys at Extreme Pressure Conditions. , 0, , .		4
52	High pressure structural study of samarium doped CeO2 oxygen vacancy conductor — Insight into the dopant concentration relationship to the strain effect in thin film ionic conductors. Solid State lonics, 2016, 292, 59-65.	1.3	4
53	Anomalous Conductivity in the Rutile Structure Driven by Local Disorder. Journal of Physical Chemistry Letters, 2019, 10, 5351-5356.	2.1	4
54	Real time study of grain enlargement in zirconium under room-temperature compression across the α to ω phase transition. Scientific Reports, 2019, 9, 15712.	1.6	4

NENAD VELISAVLJEVIC

#	Article	IF	CITATIONS
55	Phase Transitions of Cu and Fe at Multiscales in an Additively Manufactured Cu–Fe Alloy under High-Pressure. Nanomaterials, 2022, 12, 1514.	1.9	4
56	High-pressure high-temperature phase diagram of gadolinium studied using a boron-doped heater anvil. Journal of Applied Physics, 2016, 119, .	1.1	3
57	Equation of state and thermodynamic Grüneisen parameter of monoclinic 1,1-diamino-2,2-dinitroethylene. Journal of Physics Condensed Matter, 2016, 28, 395402.	0.7	3
58	STATIC HIGH PRESSURE X-RAY DIFFRACTION OF TI-6AL-4V. AIP Conference Proceedings, 2008, , .	0.3	2
59	Containment system for experiments on radioactive and other hazardous materials in a Paris-Edinburgh press. Review of Scientific Instruments, 2015, 86, 113904.	0.6	2
60	Structural Changes in Liquid Lithium under High Pressure. Journal of Physical Chemistry B, 2020, 124, 7258-7262.	1.2	2
61	Multi-phase equation of state of ultrapure hafnium to 120 GPa. Journal of Physics Condensed Matter, 2022, 34, 055401.	0.7	2
62	Strength of tantalum to 276 GPa determined by two x-ray diffraction techniques using diamond anvil cells. Journal of Applied Physics, 2022, 131, 015905.	1.1	2
63	Phase transitions in high-purity zirconium under dynamic compression. Physical Review B, 2022, 105, .	1.1	2
64	EQUATION OF STATE FOR TI-BETA-21S. , 2008, , .		1
65	STRUCTURAL PHASE STABILITY IN GROUP IV METALS UNDER STATIC HIGH PRESSURE. , 2009, , .		1
66	In situ x-ray diffraction, electrical resistivity and thermal measurements using a Paris-Edinburgh cell at HPCAT 16BM-B beamline. Journal of Physics: Conference Series, 2014, 500, 142003.	0.3	1
67	A Broadband Technique for Couplant-Corrected Pulse-Echo Measurements in a Large Volume Pressure Cell. , 2018, , .		1
68	Volume collapse phase transitions in cerium-praseodymium alloys under high pressure. High Pressure Research, 2018, 38, 270-280.	0.4	1
69	HPCAT: A Static Compression Science Sector at the Advance Photon Source. Nihon Kessho Gakkaishi, 2019, 61, 163-167.	0.0	Ο
70	Exploring Materials Synthesis, Properties, and Metastability Thorugh Rapid (De)Compression. , 2019, , .		0